Conjugated dimers of nickel(II) octaethylporphyrin linked by extended *meso,meso*-alkynyl bridges. II.[1] Redox properties and electronic spectra of electrogenerated anions and dianions

Dennis P. Arnold,[a,*] Graham A. Heath[b] and David A. James[a,†]

[a] *Centre for Instrumental and Developmental Chemistry, Queensland University of Technology, G.P.O. Box 2434, Brisbane, Australia, 4001*
[b] *Research School of Chemistry, The Australian National University, Canberra, Australia, 0200*

This paper describes the behaviour of two suites of *meso,meso*-linked diporphyrins, namely NiOEP—C_2—X—C_2—NiOEP [where X = $(C_2)_n$, for n = 0, 1, or 2; *trans*-CH=CH; 1,4-C_6H_4 ; 1,3-C_6H_4 ; 2,5-C_4H_2S] and *trans*-NiOEP—CH=CH—Y—NiOEP [where Y = C_2 ; *trans*-C_2—CH=CH; *trans*-C_4—CH=CH]. Each $[P_2]^0$ dimer has been converted to its electrogenerated dianion, and, as far as possible, to the intervening monoanion as well. Voltammetry of these diporphyrins, and comparison with the corresponding monoporphyrin models possessing the pendant bridging unit as a *meso*-substituent, show that binuclearity *per se* adds only a small anodic shift to the normal substituent effect of the electron-withdrawing *meso*-alkyne moiety. The electronic absorption spectra of the singly and doubly reduced diporphyrins, $[P_2]^{1-}$ and $[P_2]^{2-}$, were recorded over the range 330–3200 nm by means of *in situ* spectroelectrochemistry at 233 K or below. Among the diporphyrin dianions, the distinctive spectral type already established for the C_4-bridged species is retained for all those compounds which have a triple bond directly attached to the *meso*-carbon at both ends of the bridge, except for X = 1,3-C_6H_4 in which conjugation is interrupted. The near-IR signature band of these dianions, with extinction coefficients of 10^5 M^{-1} cm^{-1} or greater, falls between 10 080 and 7900 cm^{-1} (*i.e.* >1000 nm). The frequency diminishes linearly with increasing number of triple bonds. Remarkably, $[P_2]^{2-}$ species where the linker X = *trans*-CH=CH, 1,4-C_6H_4 and 2,5-C_4H_2S have similar UV to near-IR spectra and also conform to the inverse linear frequency–distance relationship. For compounds with the longest bridges, the spectrum is dominated by just two intense bands. The dianions of the alternative diporphyrins NiOEP—CH=CH—Y—NiOEP with *trans*-ethene linkers attached to both the *meso*-carbons have a more complex Soret region, but retain the unmistakable near-IR band which shifts relatively steeply from 11 250 to 9200 cm^{-1} between Y = C_2—CH=CH and C_4—CH=CH. The position of the principal $[P_2]^{2-}$ absorption band in the near-IR region can thus be finely tuned by modification of the bridge length and composition, while retaining the familiar strong absorptivity of the porphyrin π-system.

For mixed-valence $[P_2]^{1-}$, two intense near-IR bands near 3000–5000 and 10 000 cm^{-1} are observed for all the symmetrical alkyne-linked diporphyrins (X varying as above, excluding 1,3-C_6H_4). In these odd-electron systems, the low-frequency excitation ν_1 directly maps the intrinsic frontier orbital separation due to conjugative interporphyrin coupling (*e.g.* ν_1 = 4600 and 4150 cm^{-1} for the butadiyne- and octatetrayne-bridged dimers, respectively). The optical behaviour described above, spanning three oxidation states, is shown to be consistent with a generic two-porphyrin eight-orbital model for the conjugated binuclear chromophore.

Attempts to imitate the properties of the light-harvesting apparatus and reaction centres of natural photosynthetic systems provide chemists with a fertile field for synthetic and mechanistic studies.[2] The ability of these biological systems to capture, transfer and utilise the energy of incident light depends on the unique electronic properties of arrays of cyclic tetrapyrrolic pigments held non-covalently by protein matrices. Numerous artificial assemblies of porphyrin units have been synthesized as potential mimics of parts of the photosynthetic apparatus. The prospects of using porphyrinoid pigments as components of nanoscale electronic devices rely on understanding and reproducing the exquisite control of electronic communication displayed by the natural systems. Synthetic porphyrin arrays prepared for this purpose have largely utilized covalent linkers to maintain desired geometric constraints and to control the nature and degree of electronic communication between the porphyrin π-systems.

* E-mail: d.arnold@qut.edu.au
† Present address: Department of Medicine and Physiology, Boston University School of Medicine, Boston, MA 02118, USA.

The present work is part of our research programme into diporphyrins linked by conjugated *meso*-carbon to *meso*-carbon bridges which include triple bonds. We prepared the dinickel(II) complex **1** of the dimeric ligand 1,4-bis(octaethylporphinyl)butadiyne (H_2OEP—C_4—H_2OEP),[3,4] and a series of analogues containing the divalent metal ions of cobalt, copper, zinc, palladium and platinum.[5] Recently, we reported detailed voltammetric and spectroscopic studies of the members of this series, including the UV to near-IR spectra of the electrogenerated singly and doubly reduced species.[6] The remarkably intense near-IR absorption bands discovered for the mono- and di-anions led us to propose an explanation of the origins of the characteristic spectra of the three oxidation states in terms of an empirical semiquantitative 'two-porphyrin eight-orbital' scheme.[6] We have also reported the synthesis and electronic spectra of a series of octaethylporphinatonickel(II) (NiOEP) dimers linked in the *meso*-positions by bridges comprising from two to four triple bonds only, and triple bonds in conjugation with double bonds, arenes, and heteroarenes.[1,7,8] A set of monomers with the bridging moiety as *meso*-substituent was also prepared, in

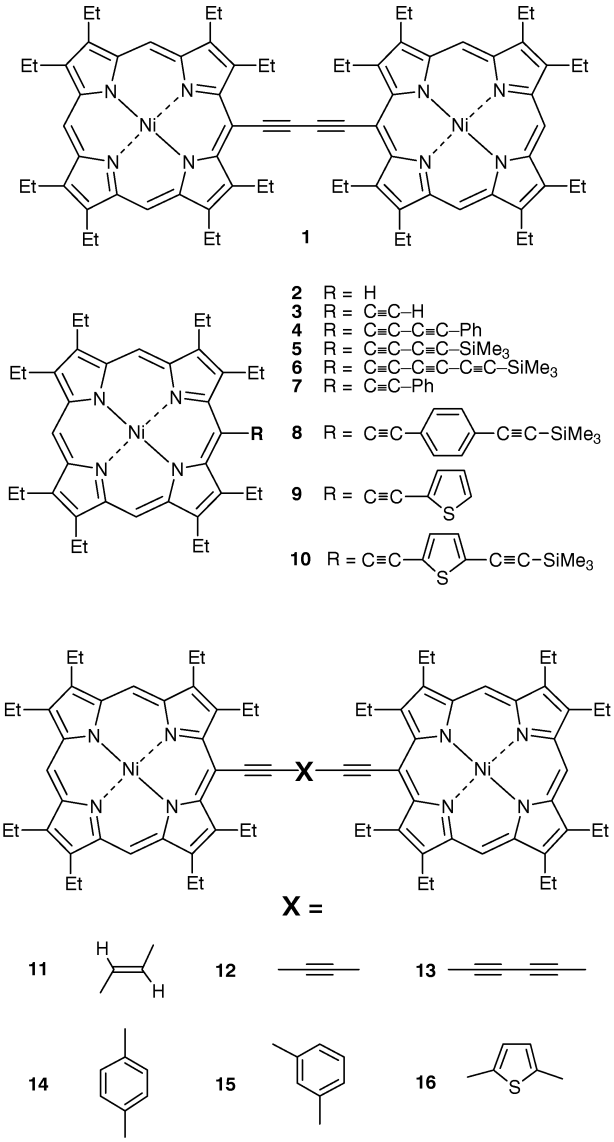

Scheme 1

order to separate the effects of the bridge acting as a substituent from those of dimerization.[1] Several other groups have studied independently alkyne-bridged oligo(porphyrin) arrays (mostly as zinc complexes), in which the porphyrins are linked by ethyne,[9] butadiyne,[9–11] phenylene–alkyne–phenylene,[12] and ethyne–arylene–ethyne units,[13] but to date our C_8-bridged derivative is the most extended strongly-coupled *meso,meso*-linked diporphyrin.

We now report the redox potentials of the second series in CH_2Cl_2 solution, together with the electronic absorption

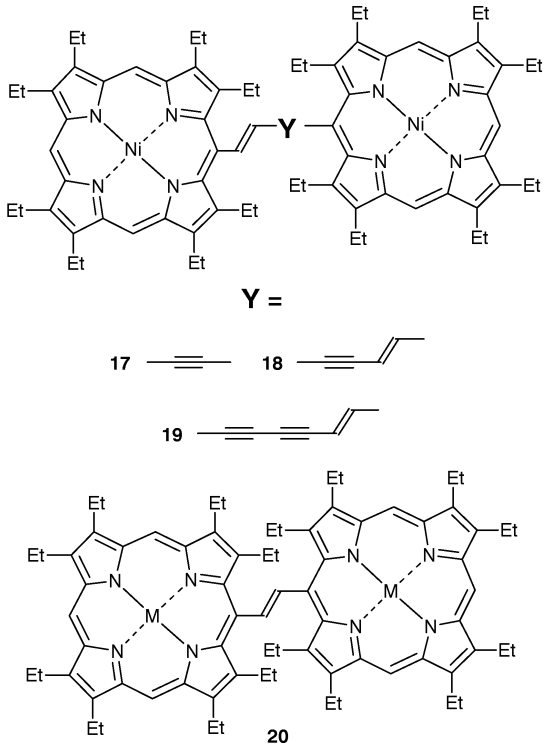

Scheme 2

spectra of the electrogenerated π-radical anions $[P_2]^{1-}$ and dianions $[P_2]^{2-}$. This suite of compounds (Scheme 1) presents a promising opportunity for fundamental studies of the ring-reduced states of dinuclear nickel(II) porphyrins. This is due to the electron-withdrawing effect of the alkynyl substituents, which shift the reduction potentials sufficiently in the anodic direction to enable spectroscopic characterization of the anions without interference from solvent- or electrolyte-induced decomposition. This contrasts with the behaviour of NiOEP itself, and NiOEP-derived monomers and dimers possessing electron-donating substituents, for which rapid chemical reactions of reduced states hinder definitive spectroscopic characterization. There has been some discussion in the literature of Ni porphyrin electrochemistry regarding whether the site of initial electron addition is the macrocycle or the metal ion.[14] These doubts are expunged for alkynyl NiOEP derivatives. The spectra of the monoanions and dianions derived from **1**, the analogous free base, and the Pd^{II} and Pt^{II} derivatives, are so similar that we can definitely conclude that Ni^{I} species are not involved.[6] In addition, the same mutual resemblance was shown for the free base and nickel(II) complex of the reduced monomer **4**.[6]

The remarkable and unmistakable spectral signatures of the 0, 1 −, and 2 − oxidation states of **1**[5,6] persist in the present

Table 1 Voltammetric data for monomers (E in V, at 293 K, *vs.* Ag/AgCl with Fc/Fc^+ at +0.55 V)

Compound	*meso*-Substituent	E^0(red)/V	E^0(ox)/V	ΔE/V
2[5]	H	−1.32[a]	0.92	2.24
4[5]	C_4—Ph	−1.04	0.97	2.01
	C_4—Ph[b]	−1.15	0.85	2.00
5	C_4—$SiMe_3$	−1.05	0.96	2.01
6	C_6—$SiMe_3$	−1.00	0.96	1.96
7	C_2—Ph	−1.16	0.91	2.07
8	C_2—1,4-Ph—C_2—$SiMe_3$	−1.15	0.91	2.06
9	C_2—Th	−1.09	0.91	2.00
10	C_2—2,5-Th—C_2—$SiMe_3$	−1.05	0.91	1.96

[a] Irreversible. [b] From ref. 15, measured by differential pulse voltammetry, Pt electrode, in CH_2Cl_2, 0.1 M Bu_4NClO_4, *vs.* Ag/AgCl.

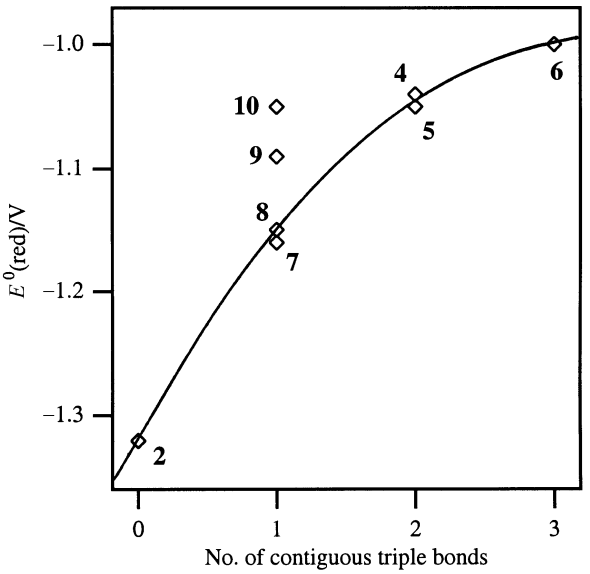

Fig. 1 Relationship between first reduction potential and the number of contiguous triple bonds in the *meso*-substituent C_n—R for monomeric NiOEP derivatives [R = H (**2**), $SiMe_3$ (**5**, **6**), Ph (**4**, **7**), Ph—C_2—$SiMe_3$ (**8**)]. Data for R = Th (**9**) and Th—C_2—$SiMe_3$ (**10**) are shown for comparison. The curve is intended only to define the empirical relationship

series of dimers, although they are systematically modified by variation of the bridging unit, as demonstrated in this work. Consideration of the progression in electrode potentials and the pattern of optical spectra enables us to draw some general conclusions regarding the effects of bridge length and composition on the extent of electronic communication between the chromophores in the dimers. This knowledge is of prime importance in formulating the broad principles (as yet undetermined) by which the utility of these and similar compounds in light-harvesting or nanoelectronic applications can be assessed.

Results

Voltammetry

The cyclic voltammograms of the *monomers* in CH_2Cl_2 revealed no unexpected features. The compounds are all easier to reduce than unsubstituted NiOEP, but their oxidation potentials are about the same as for NiOEP. The data are collected in Table 1. We did not investigate any redox steps beyond the first. This reduction for all the alkyne-substituted monomers is fully reversible, in contrast to the behaviour of NiOEP. The monoanion of the latter undergoes a chemical reaction in the Bu_4NPF_6–CH_2Cl_2 medium, resulting in a re-oxidation wave at about −0.4 V.[16] This may be due to a nickel(III) species resulting from oxidative addition of solvent or electrolyte to the metal, or to a nickel(II) phlorin complex.[16]

The data in Table 1 for monomers **2** and **4**–**10** show a number of trends related to the nature of the *meso*-substituent. A plot of E^0(red) with respect to the number of contiguous triple bonds is one logical and convenient way to approach the data, as shown in Fig. 1. The comparison of NiOEP (**2**) with **7** (as a substitute for the rather unstable **3**) and **4**/**5**, and then **5** with **6**, shows that more triple bonds make the ring reduction systematically easier, while the oxidation potentials (Table 1) vary less markedly over the same set of compounds. Thus the important parameter, the electrochemical HOMO–LUMO gap ΔE [measured by E^0(ox) − E^0(red)], contracts considerably as the number of contiguous triple bonds in the *meso*-substituent increases. In the pairs **7**/**8** and **9**/**10**, the additional but non-contiguous triple bond transmits its anodic shift of the reduction potential better across the 2,5-thienylene moiety than across the 1,4-phenylene group. This is a familiar situation due to the lower aromaticity of thiophene compared to benzene, and the former has a greater ability to conjugate with substituents and act as an electron source, sink or conduit. This is borne out by the comparison of **7** with **9** (and of **8** with **10**), which shows that the thiophene in itself is acting as a better electron-accepting substituent, accounting for an anodic shift of 70 mV (**7**/**9**) and 100 mV (**8**/**10**). We note for later reference that the reduction potential for **7** is *ca.* 110 mV less negative than that for *meso*-vinylNiOEP.[17]

In the *dimers*, the presence of two adjoining porphyrin rings suggests the possibility of the existence of mixed-valence states arising from the addition to, or abstraction from, the extended π-system of just one electron per dimer molecule. For the reductions of the four-coordinate M^{II} complexes analogous to **1**, we found that mixed-valence monoanions could be characterized by voltammetry and spectroelectrochemistry for several members, namely Ni_2, Pd_2, Pt_2, Cu_2, and Ni/Zn.[5,6] In the voltammetry, there was an observable gap between the first and second reductions, and between the first and second oxidations. In fact the oxidative splitting is larger than the reductive one, consistent with the different character of the HOMO and LUMO. Unfortunately, the oxidations are associated with complex voltammetric behaviour, probably

Table 2 Voltammetric data for dimers in CH_2Cl_2 (E in V, *vs.* Ag/AgCl, with Fc/Fc^+ at 0.55 V)[a]

		293 K			233 K		
Compound	Bridge	E^0(red)/V	E^0(ox)/V	ΔE/V	E^0(red)/V	E^0(ox)/V	ΔE/V
1[5]	C_4	−1.01	0.92, 1.04	1.93	−0.93, −1.03	0.86, 1.03	1.79
11	C_2—CH=CH—C_2	−0.95	0.93, 1.00	1.88	−0.90, −0.95	0.87, 1.01	1.77
13	C_8	−0.92	0.89, 0.97	1.81	**−0.92**	**0.84, 1.05**	**1.76**
14	C_2—1,4-Ph—C_2	−1.10	0.91, 0.96	2.01	−1.08	0.83, 1.00	1.91
15	C_2—1,3-Ph—C_2	−1.10	0.96	2.06	−1.10	0.89, 1.01	1.99
16	C_2—2,5-Th—C_2	−1.05	0.89, 0.99	1.94	−1.00	0.85, 1.10	1.85
17	C_2—CH=CH[b]	−0.88	0.87, 1.04[c]	1.75			
18	CH=CH—C_2—CH=CH[b]	−0.81	0.79, 0.94[c]	1.60			
19	CH=CH—C_4—CH=CH[b]	−0.82	0.91, 0.96[c]	1.73			

[a] The designated E^0 values are defined by the ac peak potentials (or the means of the forward and reverse ac peak potentials); ΔE is defined as E^0(ox1) − E^0(red1), except where the individual reduction waves were not resolved, in which case the average ac peak potentials were used. [b] Low-temperature data not determined. [c] Irreversible.

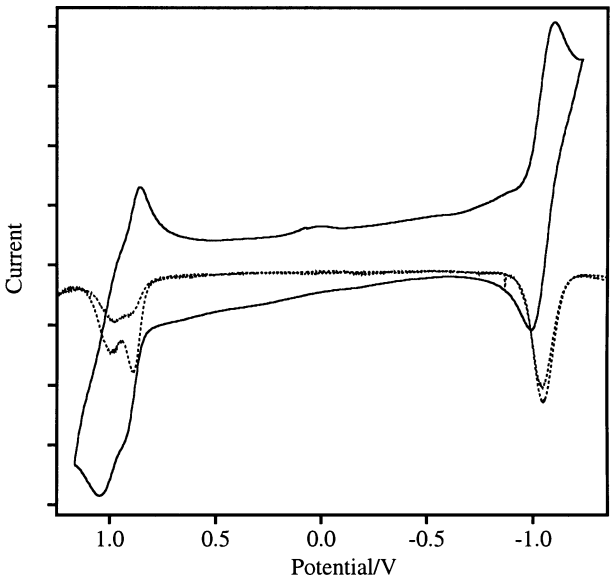

Fig. 2 Cyclic (solid line) and ac (dotted lines) voltammograms for thiophene-linked dimer **16** at 293 K

due to aggregation, and the cations are also unstable under spectroelectrochemical conditions, and could not be characterized.[5,6] In these derivatives, the largest voltammetric separation between the first and second reductions was found for the heterobimetallic Ni/Zn complex, as expected. Of the homobimetallic complexes, the dinickel species **1** has the largest gap, *ca.* 100 mV.[5,6] The significance of the modest 'mixed-valence voltammetric splitting' was analysed in detail in our earlier paper,[6] and we will return to this point in the Discussion below. In view of the above, in the present study we deal only with the reduction products, and only with nickel complexes (**11**–**19**), in anticipation that these afford the best chance of observing and characterizing the mixed-valence diporphyrin anions. Moreover, of the butadiyne-bridged compounds, the Ni_2 derivative is the most accessible and the

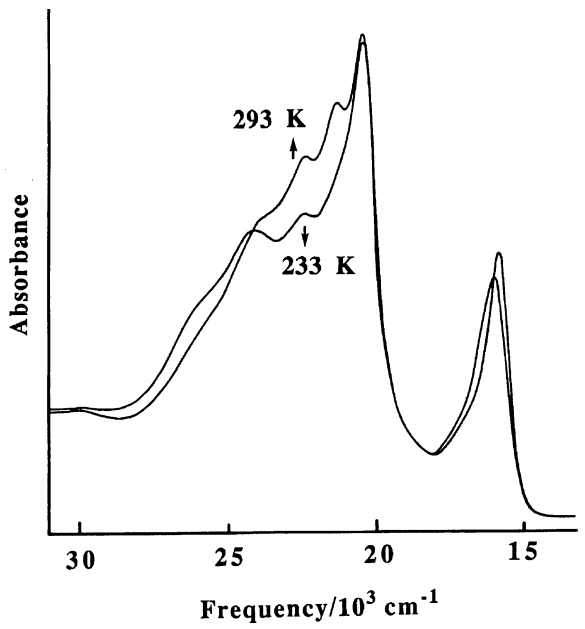

Fig. 3 Temperature dependence of the electronic absorption spectrum of the octatetrayne-linked dimer **13** in CH_2Cl_2–0.5 M Bu_4NPF_6

easiest to handle experimentally owing to its higher solubility and lesser tendency to aggregate than the analogous Cu_2 and Zn_2 complexes.[5,6]

The results of room-temperature (293 K) voltammetry for the dimers **1**, **11**, and **13**–**19** are given in Table 2. Low-temperature (233 K) data are also included except for dimers **17**–**19**, for which at 233 K, the waves representing the Faradaic couples are shallow and poorly differentiated from the baseline current. Typical cyclic and ac voltammograms are shown for dimer **16** in Fig. 2. For all dimers, the reductions were not resolved into two successive processes at 293 K, and a single $2e^-$ wave was observed. Apart from **1**, only **11** showed resolution of the reductions even at 233 K. In contrast, in all cases except the *meta*-isomer **15**, the first two *oxidation* waves were separated. In Table 2, the peak of the ac wave is quoted where the processes were unresolved. The shapes of the cyclic ac and dc scans are as expected for reversible, diffusion-limited processes, and are indifferent to initiation point (if selected within the electro-inactive window), scan direction, and number of scans. In a qualitative sense, the splitting of red1 and red2 appears to be inversely related to the length of the bridge, *e.g.*, **1** (100 mV) → **11** (50 mV) → **13** (unresolved). Within each comparative pair comprising a given dimer and its model monomer with the pendant bridge unit as substituent, there is, at most, only a small decrease in ΔE upon dimerization. This is seen in comparisons at 293 K of **1** with **5** (contraction 80 mV), **14** with **8** (50 mV), and **16** with **10** (20 mV) (Tables 1 and 2). Thus, in comparisons of NiOEP with its *meso*-bridged dimers, the major contributor to the contraction of the electrochemical HOMO–LUMO gap is the LUMO-stabilizing effect of the alkynyl substituent.[6]

It is interesting to compare the three *meso*-ethenyl dimers **17**–**19** with the rest of the series. These species all have a smaller electrochemical HOMO–LUMO gap than any of the dimers with exclusively triple bonds connected at the *meso*-positions. It has been noted before that the *trans*-ethenyl-linked system **20** (M = H_2, Ni), exhibits a remarkably narrow ox/red gap (< 1.5 V).[17,18] The reasons for this are not entirely clear at present, but appear to be due to the existence of a fast equilibrium involving one or more conformers in which the ethenyl and at least one of the porphyrin π-systems are near-coplanar. Such conformers may possess delocalized inter-porphyrin bonding, leading to unusual voltammetric and spectroscopic behaviour.[19] In the lowest energy conformer calculated by molecular mechanics,[19] and indeed in the conformation observed in the solid state,[20] the bridging double bond lies almost orthogonal to the porphyrin rings, which are themselves mutually parallel. This point will be discussed in a future publication.[21] Further analysis of the redox potentials of **17**–**19** is not warranted because we do not have the data for model monomers with the whole bridging unit as *meso*-substituent, but it should be noted that a simple vinyl substituent has only a modest effect on the redox potentials [E^0(red1) = −1.27 V, ΔE = 2.13 V].[17]

Electronic spectra of electrogenerated dimer anions and dianions

The electronic spectra of the *neutral* dimers were described in our synthetic paper.[1] The electronic spectra of the reduced states of conjugated alkyne-linked NiOEP dimers were established with reference to **1** in our previous papers.[5,6] The reduced monomer **4** was also described therein. The new dimers **11**, and **13**–**19** proved to be amenable to study using low-temperature (213–233 K) thin-layer spectroelectrochemistry. We obtained spectra of excellent quality over the extreme range from the mid-IR (3125 cm^{-1}) to the UV (33 000 cm^{-1}) for the dianions of all compounds. Even for C_6-bridged **12**, obtained as an inseparable 50 : 50 mixture with **1**, we were able to identify the major diagnostic near-IR band of its

Table 3 Major absorption bands of mono- and dianions of dimers[a]

		ν_{max}/cm^{-1}						
		Monoanions		Dianions				
Compound	Bridge					Band C	Band B	Band A
1[5,6]	C_4	11460	4600	25100s	23800s	22450	18760b	10080
11	C_2—CH=CH—C_2	10450	4450	25200		21800	18500b	9600
12	C_6[b]							9100
13	C_8[c]	11100	4150	25000s	23700s	20800b	18000s	7900[d]
14	C_2—1,4-Ph—C_2[c]	12450	<3125	25400		20900	17900s	8500
15	C_2—1,3-Ph—C_2[e]				20800[f]	19000s[f]	15600b[f]	11250[f]
16	C_2—2,5-Th—C_2	11450	<3125	25400		20850	18100s	8450
17	C_2—CH=CH	9850	5600	26200s	24600	21800	19000	11650
18	CH=CH—C_2—CH=CH[e]			27300	24950 22750s	21400	18550	11250
19	CH=CH—C_4—CH=CH[e]			26400s	24850	21450 20200s	17900	9200

[a] At 233 K except where noted; see text for explanation of band labels for dianions; b = broad top to peak; s = shoulder. [b] Measured on a 50 : 50 mixture of **1** and **12**. [c] At 213 K. [d] Pronounced shoulder on high-frequency side (*ca.* 9600 cm^{-1}), see Fig. 4. [e] Monoanion not observed. [f] This spectrum differs in form from the others (see text), so band labels are not relevant.

dianion, free of interference, although higher-frequency bands were obscured by overlap with bands of $[\mathbf{1}]^{2-}$. In addition, for some species with a sufficient thermodynamic gap between E^0(red1) and E^0(red2), namely **11**, **13**, **14**, **16**, and **17**, we also identified some characteristic bands for the intermediate mixed-valence monoanions. Gradual approach to the red1/red2 midpoint potential sometimes achieves this resolution, even when voltammetry cannot separate the closely grouped successive couples.

The optical spectra were all recorded at low temperature in order to increase the longevity of these very reactive species. In our earlier work, we drew attention to the temperature-dependence of the spectra of the neutral dimetallic derivatives of **1**.[6] In the case of **1**, lower temperatures intensified the lowest energy Soret component relative to that of its next-highest energy neighbour.[6] This change is possibly related to the populations of planar and non-planar conformers.[10] Similar effects are found in the present set of compounds, particularly for **11**, **13**, **14** and **16**. Indeed for **13** and **14**, it is important to note that lowering the temperature to 233 K or below reveals the typical appearance of conjugated alkyne-bridged dimers,[1,9,10] whereas the profiles of the Soret bands for **13** and **14** at room-temperature appeared at first sight to be out of place in the series.[1] Fig. 3 shows the effect of cooling a solution of the C_8-bridged dimer **13** from 293 to 233 K. The succession of bands of decreasing intensity from low to high energy resolves to a spectrum very like those of the archetype butadiyne **1** and the related set **11**, **14** and **16** at similar temperatures.[1]

The frequencies of the major bands in the spectra of the mono- and di-anions are listed in Table 3. We begin by presenting the results for the doubly reduced species, because spectra are available for the whole series. Although there are clearly numerous transitions apparent as maxima and shoulders in the dianion spectra, we have selected three apparently conserved bands for discussion. These have been arbitrarily labelled bands 'A', 'B', and 'C', from low to high energy, to facilitate analysis (Table 3). Note that we do not attach any particular theoretical significance to these labels at this stage, or assert that the correct band selection is self-evident in every case.

The spectra of the dianions are displayed in Fig. 4. They are arranged so that compounds with comparable numbers of carbons in the conjugation pathway lie side-by-side in the panels, with bridge length increasing down each column. As explained above, the full-range spectrum of C_6-bridged **12** is not available, and in its place between C_4 (**1**) and C_8 (**13**), we have substituted C_6H_2 (**11**). The evolution of these spectra during electrolysis from monoanion to neutral species, and from dianion to monoanion are shown for **11** in Fig. 5 and 6, respectively. The results were similar for **11**, **13**, **16**, and **17**, and these four derivatives display essentially the same behaviour as that well-established for the butadiyne **1**.[5,6] That is to say, the dianion spectrum consists of a modified 'Soret region', spanning 16000–28000 cm^{-1}, and an intense band near 10000 cm^{-1}, whose frequency and appearance depend on the structure of the bridge (see below). The shape of the Soret envelope is also subtly modified by the bridge structure and progressively simplified as Fig. 4 is descended. We draw attention in particular to the remarkable apparent simplicity of the spectra of the dianions of the *p*-phenylene and 2,5-thienylene dimers **14** and **16**, shared perhaps to a lesser extent by octatetrayne **13**. The extinction coefficients shown in Fig. 4 were derived by comparison of the final dianion spectra with the intensities of the bands in the neutral starting compounds, including thermal solvent contraction effects. The ε values are estimated to be accurate to within about 10%. The prominent near-IR bands found for all the dianions are of comparable intensity to the Soret bands of the neutral compounds, *i.e.*, $\varepsilon > 10^5\ M^{-1}\ cm^{-1}$, reaching $1.5 \times 10^5\ M^{-1}\ cm^{-1}$.

For three structural variants, namely *m*-phenylene **15**, hexadienynediyl **18**, and octadienediynediyl **19**, there was no spectroscopic evidence for the presence of the intermediate monoanions, and the reverse progressions from dianion to neutral dimer exhibited remarkably clean isosbestic points, as shown in Fig. 7 for **18**. The spectra of the dianions of **18** and **19** still conform to the pattern established by the dimers **1**, **11**–**14**, **16** and **17**, *i.e.*, they display the collapsed and split Soret region, and the *intense* band near 11000 cm^{-1}. Remarkably, the spectrum of the dianion of **15** is almost identical to that of the comparable monomer **4**.[6] The spectrum of $[\mathbf{15}]^{2-}$ is therefore essentially a superposition of two monomeric alkynyl-NiOEP monoanion units, especially with respect to the low intensity of the radical anion marker band near 11000 cm^{-1}.

Considering now the spectra of the monoanions, we first recall that the spectrum of $[\mathbf{1}]^{1-}$ displays a Soret region of diminished intensity compared with that of the neutral compound, and also has two prominent bands in the near-IR region, at 11460 and 4600 cm^{-1} (Table 3 and refs. 5,6). Because of the unavoidable disproportionation of $[P_2]^{1-}$ to $[P_2]^0$ and $[P_2]^{2-}$, the Soret bands for the monoanions

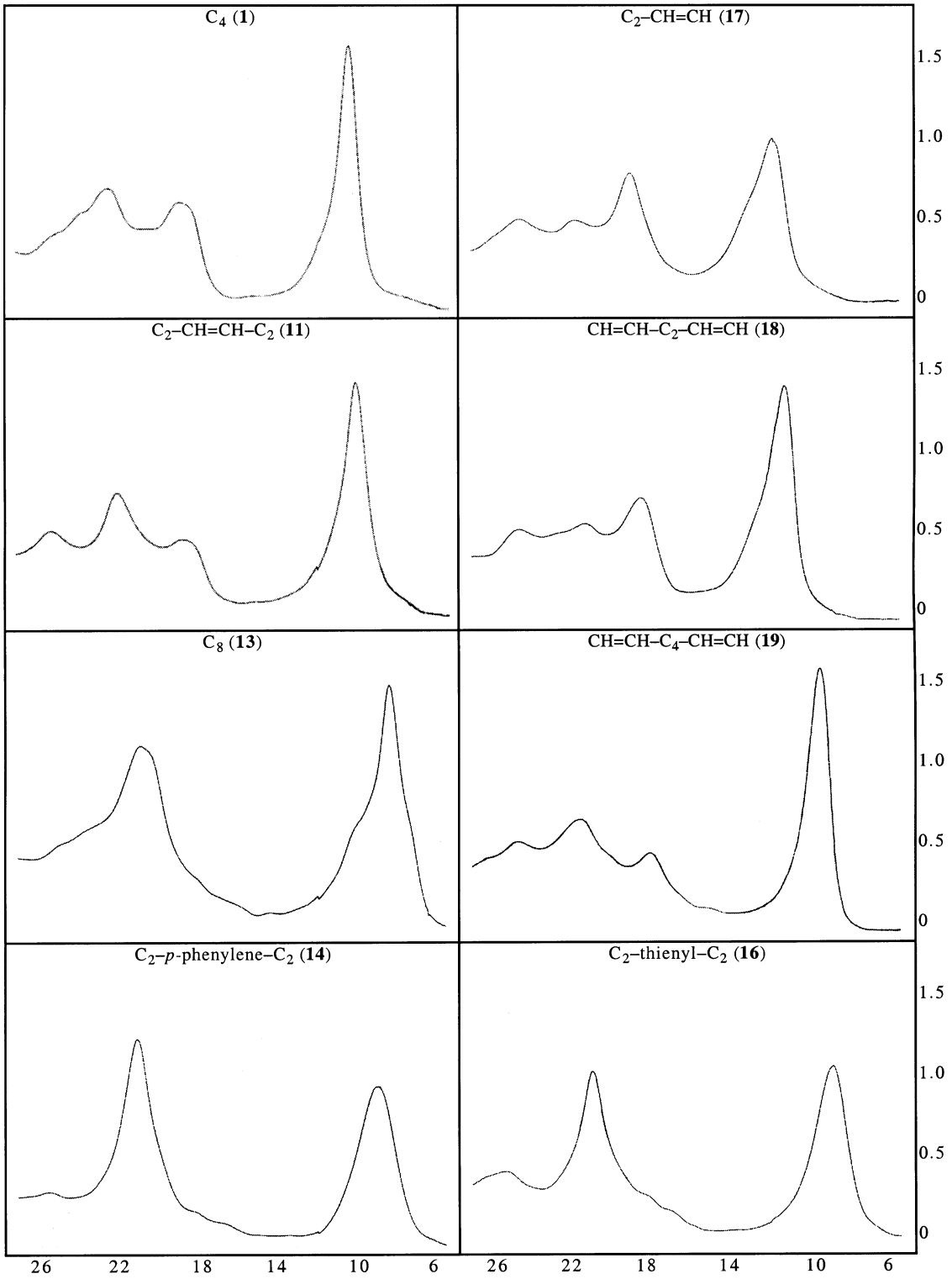

Fig. 4 Comparison of the UV to near-IR spectra of the dianions of the diporphyrins recorded in the OTTLE cell at temperatures $\leqslant$233 K (see Table 3). The common horizontal scale is in frequency/10^3 cm^{-1}, and the vertical scales are in $\varepsilon/10^5$ M^{-1} cm^{-1}

cannot readily be distinguished except in the case of $[\mathbf{1}]^{1-}$.[5,6] However, in the near-IR region, two characteristic bands of similar height near 11 000 cm^{-1} and 5000 cm^{-1} are unobscured, and these are the data given for monoanions in Table 3. We have not listed absolute intensities in the Table, but internal comparisons with the dianions (Fig. 4–6) indicate extinction coefficients in the vicinity of 50 000 M^{-1} cm^{-1}. For $[\mathbf{13}]^{1-}$, the spectral profile in the near-IR region is almost indistinguishable from that presented for $[\mathbf{1}]^{1-}$,[5,6] which in turn closely resembles that shown for $[\mathbf{11}]^{1-}$ in Fig. 5 and 6. For $[\mathbf{14}]^{1-}$ and $[\mathbf{16}]^{1-}$, the maximum of the lowest-energy absorption is apparently just beyond the limit of our spectrometer (3125 cm^{-1}), although the high-frequency edge of the band clearly extends into the observable range. Indeed for **16**, the spectral progression (Fig. 8) in the region from 15 000 cm^{-1} to the low-frequency limit strongly mimics that of **13**, even to the extent that the isosbestic points associated with the $[P_2]^{1-}/[P_2]^{2-}$ interconversion appear at 10 500 and 6000 cm^{-1} for both compounds. Thus the pattern of characteristic near-IR bands established for butadiyne-bridged diporphyrin monoanions is maintained in the present series, notably including those compounds which include *p*-phenylene and

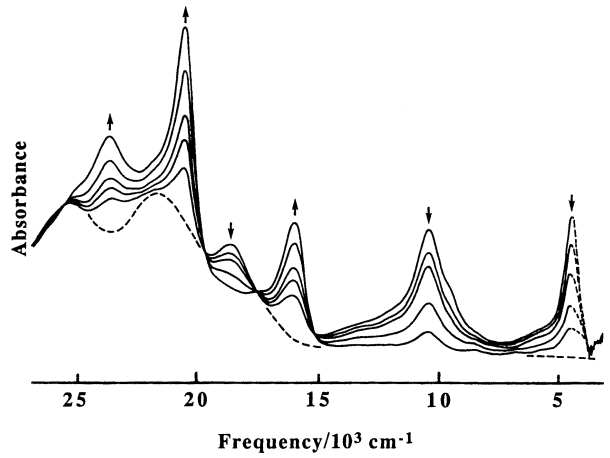

Fig. 5 Spectral evolution during electrolysis of $[\mathbf{11}]^{1-}$ to $[\mathbf{11}]^{0}$ at 233 K

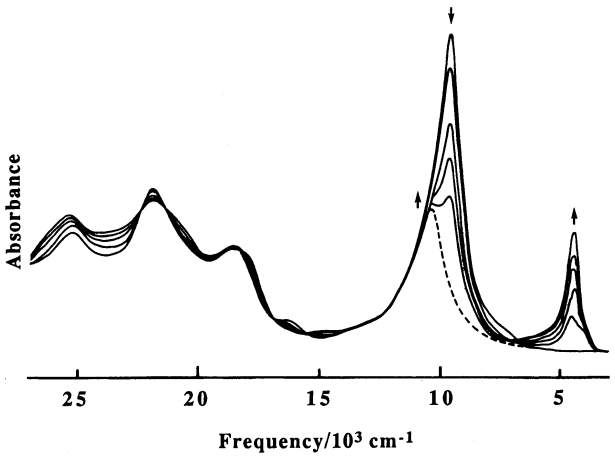

Fig. 6 Spectral evolution during electrolysis of $[\mathbf{11}]^{2-}$ to $[\mathbf{11}]^{1-}$ at 233 K

2,5-thienylene units. Compound **17**, with the asymmetric enyne linker, has its lowest-energy monoanion marker band broadened and blue-shifted by 1000 cm^{-1} compared with that of $[\mathbf{1}]^{1-}$, an observation that will be addressed below.

Discussion

In our previous paper we explained the electronic spectra of $[\mathbf{1}]^{0}$, $[\mathbf{1}]^{1-}$, and $[\mathbf{1}]^{2-}$ (and their analogues with other metal ions) in terms of a semi-quantitative 'two-porphyrin eight-orbital' scheme appropriate to the dumbbell-like binuclear chromophore.[6] Fig. 9 shows a generic eight-orbital manifold; the energetic spacing obviously differs in detail from case to case, and among the three oxidation states. In this manifold, the symbols differentiate molecular orbitals subject to ring–ring interaction *via* the bridge π-system (**x**) from those which are formally non-bonding between the porphyrins (**y**). The *x*-axis is aligned with the bridge, and hence with the long axis of the extended molecule. Central to the present work is the proposal that band A, the intense near-IR band for the dianions, represents the new 'upper-storey' frontier orbital transition $(\mathbf{x}_u^*)^2(\mathbf{x}_g^*)^0 \rightarrow (\mathbf{x}_u^*)^1(\mathbf{x}_g^*)^1$, labelled ν_1 in Fig. 9. The neutral closed-shell precursor has eight electrons in the interacting **x** frontier orbitals, so that $[P_2]^0$, $[P_2]^{1-}$, and $[P_2]^{2-}$ are henceforth designated respectively 8e, 9e, and 10e species.

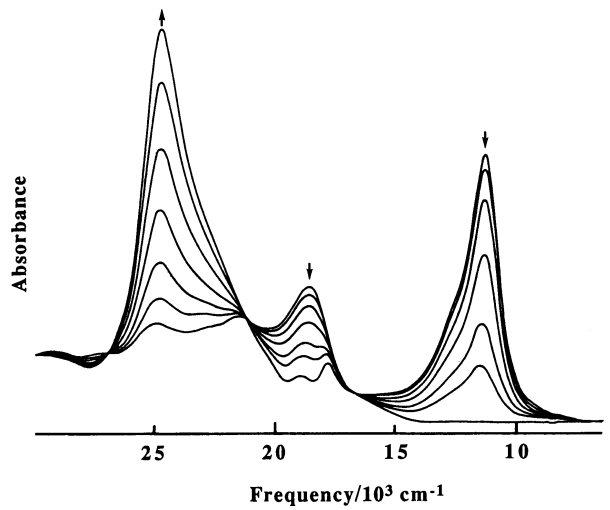

Fig. 7 Spectral evolution during electrolysis of $[\mathbf{18}]^{2-}$ to $[\mathbf{18}]^{0}$ at 233 K

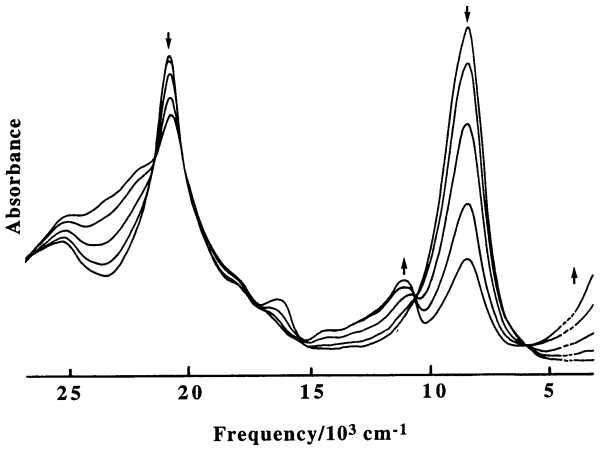

Fig. 8 Spectral evolution during electrolysis of $[\mathbf{16}]^{2-}$ to $[\mathbf{16}]^{1-}$ at 233 K

There have been some efforts already to use molecular orbital computations to quantify the electronic structure of *neutral* (8e) dimers linked by butadiyne bridges, and to rationalize their novel electronic spectra. Anderson and co-workers used INDO/MRD-CI and INDO/SCI methods for a C_4-bridged Zn_2 dimer,[22] while our colleagues applied density functional theory (DFT) to the porphine analogue of **1**.[23] There are also published DFT calculations on 1,4-bis-[10′,15′,20′-tris(trimethylsilylethynyl)porphinatozinc(II)-5′-yl]butadiyne.[24] The picture that emerges in all three treatments is qualitatively in accord with the empirically derived scheme

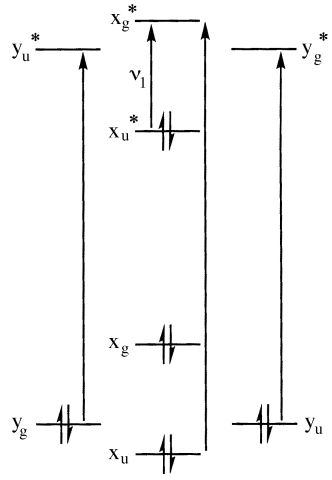

Fig. 9 A generic qualitative 'two-porphyrin eight-orbital' diagram for conjugated porphyrin dimer dianions, showing the frontier orbitals derived from the classical a_{1u}, a_{2u} and e_g^* orbitals of a symmetrical porphyrin monomer, and the long-axis polarised one-electron transitions

presented for $[P]^{2-}$ in Fig. 9. So far there have been no theoretical calculations on the *reduced* (9e and 10e) states of such dimers, the main focus of attention in the present study.

Spectra of the electrogenerated dianions

Apart from the atypical but highly informative dimer **15** described above, the dianions provide a family of closely related spectra, as shown in Fig. 4. Nevertheless, the frequencies and the relative intensities of the various absorption bands are influenced by both bridge structure and length. To assist in assessing this behaviour, Fig. 10 and 11 show the empirical variation of the frequencies of two prominent bands with respect to the distance from *meso*-carbon to *meso*-carbon across the bridge (representing the interporphyrin separation).

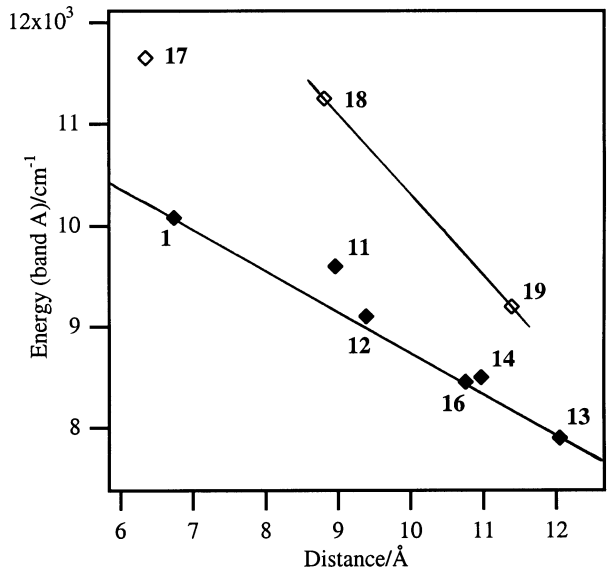

Fig. 10 Plot of the frequency of the near-IR band A *vs.* *meso*-carbon to *meso*-carbon distance (calculated). The lines join the points for **1** and **13**, and **18** and **19**, and are drawn merely to assist comparisons (see text)

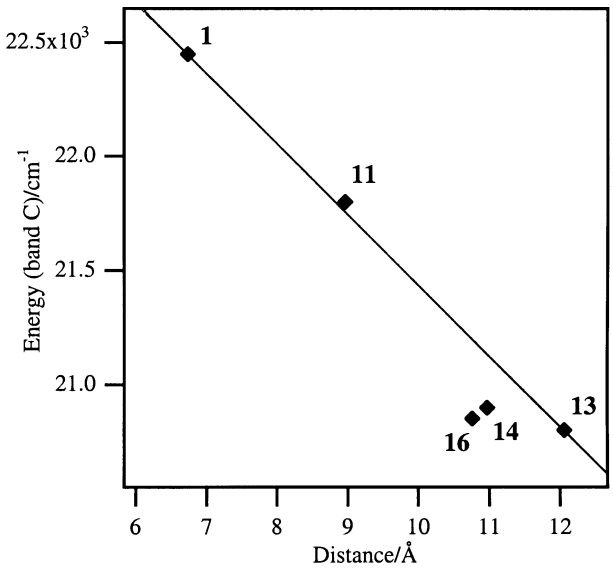

Fig. 11 Plot of the frequency of the central component of the Soret envelope, band C, *vs.* *meso*-carbon to *meso*-carbon distance (calculated). The line joins the points for **1** and **13**, and is drawn merely to assist comparisons (see text). The dimers **17**–**19** are not shown because of uncertainty in labelling the bands

The distances were estimated from molecular modelling using standard bond distances and angles for the bridge components. The frequency of band A, the near-IR signature band, is plotted in Fig. 10. We have joined the points for butadiyne **1** and octatetrayne **13** to establish a straight line defined only by the behaviour of these two archetypal yne-only species. The other compounds are then compared without prejudice against this trend. As mentioned above, the datum for hexatriyne $[\mathbf{12}]^{2-}$ is available, since its band A was clearly defined in a mixture with $[\mathbf{1}]^{2-}$. This point is gratifyingly close to the line joining **1** and **13**, so these three compounds with rigorously comparable structures and orbitals display a near-linear diminution of frequency with the number of conjugated triple bonds in the bridge. The red-shift of band A (representing ν_1 in Fig. 9) can be interpreted as a decrease in the interactive splitting between the $\mathbf{x}_u^*$ and $\mathbf{x}_g^*$ bridge-dependent molecular orbitals as the porphyrins become more remote from each other.

The other three compounds with triple bond attachments at *both* ends of the linker also lie close to the C_4—C_8 (**1**–**13**) line, despite the incorporation of non-yne units in the bridge. Thus the dianions of **11**, **14** and **16**, mimic true C_n-bridged diporphyrins. It appears that the structures which maintain the π-orbital conduit between the porphyrin *meso*-carbon-ethyne units conform to a single spectral class. There is no fundamental requirement for this to hold, especially given the loss of symmetry in **11** and **16**, and it remains to be seen how broadly this conformity is extended by synthesis of diporphyrins with a wider range of linkers.

The points for compounds with at least one *double* bond attached at the *meso*-carbon (**17**–**19**) depart from the 'yne-linked' norm in Fig. 10. Nevertheless frequencies for this subset still fall with increasing distance, and indeed the slope of the line joining the strictly analogous pair **18** and **19** is greater than that of the line joining **1** and **13**. The frequency displacement of **17**–**19** in Fig. 10 presumably reflects the rather different *meso*-substituent effect of the double bond. The same grouping is seen at a glance in the E^0 data of Table 2. The steric congestion engendered by the vinylic hydrogens and the flanking ethyl groups is expected to result in partial loss of conjugative communication between the porphyrin and the bridge. In crystals of neutral porphyrins with *meso*-vinyl substituents[25] or dimers linked by a *trans*-ethene bridge,[20] the double bond is oriented well out of the porphyrin plane. Even when the β-pyrrolic carbons are unsubstituted, the *meso*-vinyl groups adopt a dihedral angle of 36° with respect to the porphyrin plane in [5,15-divinyl-10,20-diphenylporphinato-zinc(II)$(THF)_2$].[25] However, it must be noted that the present dianions still have spectra strongly resembling those of the yne-linked dianions in overall form (Fig. 4). We conclude that the steric problems are overcome to a large extent in the dianions, the logical driving force being the formation of the interporphyrin two-electron bond embodied by the $(\mathbf{x}_u^*)^2$ level of Fig. 9.

Likewise, in the Soret region there is a systematic decrease in frequency of band C with increasing interporphyrin separation. This trend is shown in Fig. 11, and again the yne-linked compounds cluster near the line joining **1** and **13**. This band could not be located for C_6-bridged **12**, but C_6H_2-bridged **11** once again provides a well-behaved if non-rigorous mimic. It is more problematic to define the trend in band C for **17**, **18**, and **19** because the absorption seems to split in **18** and to change appearance in **19**, so these compounds have been omitted from Fig. 11. An orderly red-shift of some 1000 cm^{-1} in the adjacent *band B* is discernible for **17**–**19**.

Fig. 4 emphasises the similarity between the various dianion chromophores but also makes it apparent that the nature of the bridge has a considerable effect on the relative intensities of the characteristic bands A, B, and C. Rigorous comparisons would require the use of the oscillator strengths of individual

band components, but this is impracticable because (i) bands A and/or B sometimes have unresolved shoulders, (ii) band B is very weak in some cases, and (iii) band C for **18** and **19** is not easily defined. As seen in Fig. 4, band B, on the red edge of the Soret envelope, unequivocally diminishes in intensity as the interporphyrin distance increases. The central component of the Soret region (band C) appears to retrieve the lost intensity of band B, leading to the essentially two-band spectrum of the species with the longest bridges, *i.e.*, **13**, **14**, and **16**. To a lesser extent, the same trend is apparent for **17**–**19**. No relationship suggestive of configuration interaction (CI)[26] was found between the A : C peak-height ratio and the mean frequency (A + C)/2 or separation (A − C) of these prominent bands. Both (A + C)/2 and A − C rationally reflect the interporphyrin distance, as indicated in Fig. 10 and 11.

In summary, stepwise reduction to the dianion decisively alters the pattern of electronic bands while retaining the strong absorptivity typical of porphyrin spectra. For the set of compounds studied here, the frequencies and the relative intensities of bands in the dianion spectra can be controlled by judicious modification of the bridging unit. This culminates in bands with extinction coefficients in excess of 10^5 M^{-1} cm^{-1} displaced to beyond 10 000 cm^{-1} (>1000 nm) in the near-IR region. Indeed the dianion of **14** should be virtually transparent in the visible domain!

We suggest that, for dianions with the longest fully-conjugated bridges in the series (*i.e.*, those of **13**, **14**, **16**), the dominance of two absorption bands seen in Fig. 4 is due to the ebbing of intensity of all the 'cross transitions', *i.e.*, $\mathbf{x} \rightarrow \mathbf{y}^*$ and $\mathbf{y} \rightarrow \mathbf{x}^*$, which are necessarily short-axis (*i.e.*, *y*) polarized (*cf.* Fig. 9), whereas transitions polarized in the long-axis direction ($\mathbf{x} \rightarrow \mathbf{x}^*$ and $\mathbf{y} \rightarrow \mathbf{y}^*$) persist and gain intensity. In other words, in the sequence **1**, **11**(**12**), **13**, these cross transitions (localized on the individual porphyrins, rather than sustained *via* the bridge orbitals) become less prominent as the bridge extends, leading to progressive simplification of the Soret envelope. The neutral precursors **13**, **14** and **16** lack the two electrons filling $\mathbf{x}_\mathbf{u}^*$, which increases the number of permitted $\mathbf{y} \rightarrow \mathbf{x}^*$ transitions in this region so that multiple Soret bands persist regardless of bridge length.

In interrupted alkyne-linked species such as *m*-phenylene **15**, the spectra of both the neutral molecule and its dianion are basically those of two non-interacting porphyrins, with typically intense Soret and weak Q band profiles. The Soret band of $[\mathbf{15}]^0$ shows a very small splitting of *ca.* 550 cm^{-1}, within the expectations of through-space excitonic coupling, rather than through-bond conjugative interaction. As noted above, the turning-on of intensity in the near-IR region of the dianion spectra is clearly associated with the existence of a π-electronic conduit in the form of a conjugated bridge.

It is a curious circumstance that the spectra of our 10e dimer dianions (especially those with longer bridges) qualitatively resemble those of *neutral* oligoporphyrins linked by conjugated ethyne,[9] butadiyne,[11] or 1,4-diethynylphenylene units.[13] In these oligomers, the typical Soret/Q band profile of a monomeric porphyrin chromophore becomes heavily modified to the extent that the 'Q' band dominates an essentially two-band spectrum, as the oligomer increases in length.[11,13] The red-shift of their lowest energy band is clearly due to the cumulative (and anisotropic) bathochromic effects within the *meso*-multiporphyrin array, selectively raising π_x and lowering π_x^*. The $\pi \rightarrow \pi^*$ transitions (which were formerly near-degenerate in the parent monomer) are now completely free of CI, and their intrinsic intensity is revealed. Thus the spectra of the neutral oligomers resemble those of monomeric phthalocyanines, where the Q bands are of comparable intensity to the Soret bands.[27] Equally, the simplified spectra of our extended-bridge dianions recall the spectra of phthalocyanines. This resemblance is coincidental, because band A in the $[P_2]^{2-}$ anions is due to the 'upper-storey' excitation, $\mathbf{x}_\mathbf{u}^* \rightarrow \mathbf{x}_\mathbf{g}^*$, unrelated to the classical $a_{1u}/a_{2u} \rightarrow e_g^*$ HOMO–LUMO transitions of the neutral monomer.

Spectra and disproportionation of electrogenerated monoanions

We now consider the mixed-valence monoanions, where generally speaking two distinctive marker bands arise in the visible to near-IR spectrum as seen in Table 3. The dimer monoanions have one less electron than shown in Fig. 9, so that the leading transition ν_1 takes the form $(\mathbf{x}_\mathbf{u}^*)^1(\mathbf{x}_\mathbf{g}^*)^0 \rightarrow (\mathbf{x}_\mathbf{u}^*)^0(\mathbf{x}_\mathbf{g}^*)^1$ while ν_2 is assigned as $(\mathbf{x}_\mathbf{g})^2(\mathbf{x}_\mathbf{u}^*)^1 \rightarrow (\mathbf{x}_\mathbf{g})^1(\mathbf{x}_\mathbf{u}^*)^2$. The odd-electron population leads to cancellation of electron-correlation contributions to the excitation energy for both excitations.[6] This has the particular advantage that (unlike the situation in $[P_2]^{2-}$) ν_1 in the 9e systems directly quantifies the underlying $\mathbf{x}_\mathbf{u}^*/\mathbf{x}_\mathbf{g}^*$ orbital splitting, *i.e.*, the measured transition energy now corresponds to *twice* the resonance energy of the prevailing porphyrin/porphyrin interaction.

It is for this reason (elimination of correlation energy) that ν_1 falls from *ca.* 10 000 cm^{-1} in $[P_2]^{2-}$ to 5600 cm^{-1} or below in $[P_2]^{1-}$ (Table 3), although the underlying orbital–orbital separation is more or less constant. Initial theoretical estimates of the bridge-modulated frontier-level interaction match these definitive experimental observations remarkably well; for example, C_4-bridged $[\mathbf{1}]^{1-}$ has its ν_1 band at 4600 cm^{-1} while the MO-splitting calculated for the neutral prototype is 4000 cm^{-1}.[23]

In the light of the above, the near-IR spectra of the present bridge-extended systems in their mixed-valence 9e state have been keenly pursued. This task is complicated in the present systems by the innate tendency to disproportionation, which means that electro-generated $[P_2]^{1-}$ is inevitably accompanied by equilibrium concentrations of $[P_2]^0$ and $[P_2]^{2-}$. The origin of this somewhat unexpected propensity on the part of the electronically delocalized monoanion dimers is examined later in this section. Most importantly, C_8-bridged **13**, with the longest bridge, is seen to emulate C_4-bridged **1** in this informative oxidation state. The leading band ν_1 remains sharp and extremely intense, and is displaced only moderately (to 4150 cm^{-1}) between $[\mathbf{1}]^{1-}$ and $[\mathbf{13}]^{1-}$ while the interporphyrin separation increases from *ca.* 6.7 to 12.0 Å. The relative position and intensity of ν_2 are also preserved. We can say little of the closely related triyne monoanion $[\mathbf{12}]^{1-}$ except that its optical properties are evidently too similar to those of $[\mathbf{1}]^{1-}$ for independent resolution when mixtures of the two are reduced in the spectroelectrochemical cell.

For the wider variety of conjugated $-C_2-[X]-C_2-$ linkages incorporated in **11**, **14**, **16**, it is clear from Table 3 that $[\mathbf{11}]^{1-}$, where X = *trans*-CH=CH, most closely mimics a true yne-only bridged 9e system. This parallels the mimicry of C_6 $[\mathbf{12}]^{2-}$ by $[\mathbf{11}]^{2-}$ already noted for the 10e state. Similarly, judged by their visible to near-IR spectra, C_8 $[\mathbf{13}]^{1-}$ is largely emulated by $[\mathbf{16}]^{1-}$ where X = 2,5-thienylene, and $[\mathbf{16}]^{1-}$ in turn is largely emulated by $[\mathbf{14}]^{1-}$, where X = 1,4-phenylene. These aromatic linkers both provide an eight-carbon conjugation pathway to compare with C_8, though the characteristic electronic properties and geometries of the aromatic linkers have an important influence on the efficiency of the conduit. The ν_2 marker band is slightly raised in energy in $[\mathbf{14}]^{1-}$ and $[\mathbf{16}]^{1-}$, compared to $[\mathbf{13}]^{1-}$ (*cf.* Table 3), while ν_1 diminishes by 1000 cm^{-1} or more.

Diporphyrin **17** is unique amongst the compounds considered here (and elsewhere) by virtue of the intrinsic asymmetry of the enyne bridge. The scale of this effect may be crudely gauged from the difference in first reduction potentials of *meso*-ethenyl- and *meso*-phenylethynylNiOEP (**7**, Table 1), which we estimate to be *ca.* 110 mV in favour of the ethynylporphyrin reduction.[17] This is expected to introduce an element of porphyrin-to-porphyrin charge transfer into ν_1 for

$[\mathbf{17}]^{1-}$. In consequence, ν_1 is displaced by 1000 cm^{-1} (*ca.* 0.125 eV) compared with that in $[\mathbf{1}]^{1-}$, akin to the behaviour of the asymmetric Ni/Zn analogue of $[\mathbf{1}]^{1-}$ described elsewhere.[6]

Returning to the consideration of the symmetric systems, there is an apparent conundrum in the contrasting observations that these conjugated diporphyrins are 'strongly coupled' according to their electronic spectra, but exhibit only modest mixed-valence voltammetric splittings which diminish with increasing physical separation of the porphyrin centres.[6] We have proposed that for systems that behave in this fashion, the resonance integral quantifying the interaction between the redox centres is maintained or enhanced in the state with the potential 2e bond, compared with the hemi-bonded state.[6,28] This leaves electrostatic factors as the major contributors to the voltammetric delay between the first and second reductions. In the present series, this situation still applies. The change in red1/red2 splitting from *ca.* 100 mV for **1** to *ca.* 50 mV for **11**, and unresolved for the rest, can be attributed to a decrease in the electrostatic term because of the dispersal of the added charge over a larger system.

It is of some interest that we were unable to distinguish mixed-valence states for **18** and **19**, although the yne-linked species with comparable interporphyrin separations (**11**, **13**, **14**, **16**) did allow observation of an intermediate oxidation state under similar experimental conditions. This may be the result of enhanced interporphyrin bonding in the dianion relative to the complementary monoanion for the ene-linked compounds. The latter possibility was introduced above in relation to the geometrical inhibition of conjugation in *meso*-vinyl-substituted OEP systems. We propose that the gain in resonance energy upon conversion to the dianion overcomes the steric barrier to rotation of the double bond into coplanarity with the porphyrins. This explains three observations: (i) the electronic spectra of $[\mathbf{18}]^0$ and $[\mathbf{19}]^0$ do not have the characteristic 'strongly-coupled' yne-linked appearance,[1] (ii) the mixed-valence monoanions are unobservable, and (iii) the corresponding dianions do have the intense near-IR signature band. The dianions of the *trans*-ethene-linked dimers **20** (M = H_2, Ni) have electronic spectra of the 'non-interacting' pattern exemplified by $[\mathbf{15}]^{2-}$, *i.e.*, their near-IR bands are weaker than the bands in the Soret region.[21] This is presumably because with such a short bridge the linkage region is congested by two sets of flanking ethyl groups, thus preventing coplanarity even in the dianions. The longer bridges in **18** and **19** apparently separate the OEP units sufficiently to permit conjugation, and hence the intense signature band, to be switched on when the occupancy of $\mathbf{x}_u^*$ reaches two.

Conclusions

The archetypal electronic behaviour established for *meso,meso* butadiyne-bridged NiOEP—C_4—NiOEP (**1**) over three oxidation states is maintained in a new series of diporphyrins in which the bridge has been extended as far as eight conjugated carbons, by incorporation of additional alkyne units to form the hexatriyne and octatetrayne representatives (**12** and **13**). Analogues of the form NiOEP—C_2—X—C_2—NiOEP with a conjugated *trans*-CH=CH—, 1,4-phenylene, or 2,5-thienylene unit inserted at the midpoint of the C_4 bridge of **1** (**11**, **14**, **16** respectively) are found to mimic the true C_n yne-only systems in most respects.

In contrast, the instructive 1,3-phenylene-linked dimer **15**, where bridge conjugation is interrupted, behaves as two non-interacting porphyrin chromophores. Alternative systems *trans*-NiOEP—CH=CH—Y—NiOEP with alkene rather than alkyne connection to one of the porphyrin *meso*-carbons (Y = C_2, *trans*-C_2—CH=CH, *trans*-C_4—CH=CH, **17**–**19** respectively) form a different class in terms of their redox and spectroscopic behaviour.

We have taken a multifaceted approach to exploring the strength of electronic coupling across the bridge as a function of oxidation state, and therefore we studied the comparative electrode potentials and the UV to near-IR electronic spectra of the compounds in the oxidation states $[P_2]^0$, $[P_2]^{1-}$, $[P_2]^{2-}$. For the electronically interrupted 1,3-phenylene-bridged **15**, and for *meso*-ethene-connected **18** and **19**, the disproportionation constants of the mixed-valence monoanions are too large to permit observation of their spectra. For the rest, the two near-IR bands characterizing $[P_2]^{1-}$ were observed, notwithstanding the disproportionation equilibrium involving $[P_2]^0$ and $[P_2]^{2-}$. The lowest frequency band ν_1 for the monoanions directly defines the intrinsic frontier orbital separation which quantifies the extent of porphyrin–porphyrin coupling; ν_1 varies between *ca.* 3000 and 5600 cm^{-1}. Diporphyrin **17** is unique in possessing an asymmetric bridge, making the porphyrin termini non-equivalent, and leading to a blue-shift of ν_1 for $[\mathbf{17}]^{1-}$ compared with its C_4 relative $[\mathbf{1}]^{1-}$.

The diporphyrin dianions were characterized in all cases, and as the bridge is extended, the spectra of the *meso*-alkyne-connected species become remarkably simple, being dominated by two bands of comparable intensity. The frequency of the intense near-IR band (identified previously for $[\mathbf{1}]^{2-}$) decreases linearly with interporphyrin distance in the sequence **1**, **11**, **14**, **16**, **13**, between the limits 10 080 and 7900 cm^{-1}. The dianions of compounds **17**–**19** share the strong signature band near 10 000 cm^{-1}. In these reduced ene-linked species, there is circumstantial evidence for enhanced interporphyrin electronic coupling, which would be permitted by closer approach to coplanarity of the π-systems of the bridge and the two flanking porphyrins upon double occupancy of the frontier orbital (the former LUMO of $[P_2]^0$). More generally, the presence of undiminished or even enhanced interporphyrin bonding in the 10e dianions *versus* the 8e $[P_2]^0$ and 9e $[P_2]^{1-}$ states, leads inevitably to a small voltammetric separation between the successive redox couples.

The field of *meso*-alkyne-linked multiporphyrin arrays is now maturing, thanks to the distinctive contributions from laboratories around the world. Therien's group pioneered the use of the sterically-unencumbered 5,15-diphenylporphyrin (DPP) nucleus, and studied its dimers linked *via* C_2 and C_4 bridges in the *meso,meso*-orientation, as well as comparing these with *meso*,β-DPP/TPP and β,β-$(TPP)_2$ analogues, and also produced the first C_2-linked DPP trimer.[9] Anderson and co-workers have studied oligo(porphyrins) containing octaalkyl- or 5,15-diarylporphyrin moieties connected by *meso*-C_4- or diethynylarylene linkages,[10,11,13a,22] and Jones and co-workers have employed 1,4-diethynylphenylene units in a poly(porphyrin) chain.[13b] Although not containing alkynyl bridges, several new conjugated multiporphyrinoid arrays have recently been reported.[29]

Our own continuing contribution to developing the chemistry of the C_4—**1** prototype[3,4] lies in (i) engineering the geometric and electronic properties of the *meso-meso* bridge in NiOEP-based diporphyrins by varying the C_2—**X**—C_2 linkage,[1] (ii) systematically varying the nature of the embedded four-coordinate metal ions[5,6] (M = Ni, Pd, Pt, Co, Cu, Zn, 2H), and (iii) pursuing alternative oxidation states of the diporphyrin, as described herein and elsewhere.[5,6] The discovery of the remarkable optical properties of the 9e and 10e diporphyrin anions (made possible by voltammetric and spectroelectrochemical studies) particularly differentiates our work. The reduced dimers represent a new class of porphyrinoid pigments, worthy in their own right of continued elaboration by synthetic, spectroscopic and theoretical studies. Investigation of these novel chromophores is still in its infancy; we look forward to wider discussion of the empirical data and of the qualitative proposals on electronic structures which we have advanced to account for their properties.

Experimental

The syntheses of the relevant compounds have all been described previously.[1] Hexatriyne dimer **12** was obtained only as a 50 : 50 mixture with butadiyne **1**.[1] Dichloromethane was pre-dried over KOH pellets and distilled from CaH_2 under N_2 immediately before use. Electrolytes (Bu_4NPF_6 and Bu_4NBF_4) were purified by repeated recrystallization from absolute ethanol and vacuum drying.

Voltammetry

A standard three-electrode configuration was used, with a Pt button working electrode and a Pt wire counter electrode. The reference electrode comprised a silver wire coated with silver chloride separated from the working solution by two fritted jackets. The internal chamber containing the wire was filled with 0.05 M Bu_4NCl–0.45 M $Bu_4NPF_6(BF_4)$, and the external chamber contacting the working solution was filled with 0.5 M $Bu_4NPF_6(BF_4)$, all in CH_2Cl_2. The working solution was pre-purged and subsequently protected with N_2. The voltammetry of the monomers was carried out at Queensland University of Technology, in CH_2Cl_2 containing 0.5 M Bu_4NPF_6, using a PAR model 273A system linked to a desktop computer. The dimers were studied at the Australian National University (ANU) in CH_2Cl_2 containing 0.5 M Bu_4NBF_4, using a PAR model 170 system linked to an Apple Macintosh LC630 computer *via* a Maclab (AD Instruments) interface. The ANU system used a jacketed glass cell whose temperature was controlled using a Lauda RL6 circulating refrigerated methanol bath. The solution temperature was monitored by a thermocouple probe immersed in the solution. Electrode potentials are reported (Table 2) using ferrocene as internal standard [$E^0(ox) = +0.55$ V]. The stated E^0 values were operationally defined by the ac peak potentials (or the mean of the forward and reverse ac peak potentials in some cases where these were not precisely coincident).

Spectroelectrochemistry

These experiments were conducted at ANU using a cryogenically controlled optically transparent thin-layer electrogenerative (OTTLE) cell, as described elsewhere.[30] Electrolysis was usually carried out at temperatures of 233 K, at -1.4 V, and continued until the spectrum ceased to change and the current stabilized. The potential was then gradually adjusted in the anodic direction and spectra were recorded at appropriate intervals across the region 3125–33 000 cm^{-1}. The conversions of dianions to monoanions and thence to the neutral species were followed to the extent allowed by the comproportionation constants. The observation of stable and reproducible isosbestic points, and the regeneration of the initial spectrum, were taken as evidence of the chemical reversibility of the reductions.

Acknowledgements

We thank the Australian Research Council for partial support of this work, and The Institute of Advanced Studies, ANU, for a Collaborative Grant. D. A. J. acknowledges the support of an Australian Postgraduate Award.

References

1 Part I: D. P. Arnold and D. A. James, *J. Org. Chem.*, 1997, **62**, 3460.
2 See, for example: M. O. Senge, M. G. H. Vicente, K. R. Gerzevske, T. P. Forsyth and K. M. Smith, *Inorg. Chem.*, 1994, **33**, 5625, and references therein; G. McDermott, S. M. Prince, A. A. Freer, A. M. Hawthornthwaite-Lawless, M. Z. Papiz, R. J. Cogdell and N. W. Isaacs, *Nature* (*London*), 1995, **374**, 517; R. Wasielewski, *Chem. Rev.*, 1992, **92**, 435; T. Pullerits and V. Sundström, *Acc. Chem. Res.*, 1996, **29**, 381.
3 D. P. Arnold, M. Mahendran and A. W. Johnson, *J. Chem. Soc., Perkin Trans. 1*, 1978, 366.
4 D. P. Arnold and L. J. Nitschinsk, *Tetrahedron*, 1992, **48**, 8781.
5 D. P. Arnold and G. A. Heath, *J. Am. Chem. Soc.*, 1993, **115**, 12197.
6 D. P. Arnold, G. A. Heath and D. A. James, *J. Porphyrins Phthalocyanines*, 1998, in press.
7 D. P. Arnold and L. J. Nitschinsk, *Tetrahedron Lett.*, 1993, **34**, 693.
8 D. P. Arnold, D. A. James, C. H. L. Kennard and G. Smith, *J. Chem. Soc., Chem. Commun.*, 1994, 2131.
9 V. S.-Y. Lin, S. G. DiMagno and M. J. Therien, *Science*, 1994, **264**, 1105; P. J. Angiolillo, V. S.-Y. Lin, J. M. Vanderkooi and M. J. Therien, *J. Am. Chem. Soc.*, 1995, **117**, 12514; V. S.-Y. Lin and M. J. Therien, *Chem. Eur. J.*, 1995, **1**, 645.
10 H. L. Anderson, *Inorg. Chem.* 1994, **33**, 972.
11 H. L. Anderson, S. J. Martin and D. D. C. Bradley, *Angew. Chem., Int. Ed. Engl.*, 1994, **33**, 655; P. N. Taylor, J. Huuskonen, G. Rumbles, R. T. Aplin, E. Williams and H. L. Anderson, *Chem. Commun.*, 1998, 909.
12 S. Prathapan, T. E. Johnson and J. S. Lindsey, *J. Am. Chem. Soc.*, 1993, **115**, 7519; R. W. Wagner and J. S. Lindsey, *J. Am. Chem. Soc.*, 1994, **116**, 9759; R. W. Wagner, T. E. Johnson, F. Li and J. S. Lindsey, *J. Org. Chem.*, 1995, **60**, 5266; K. K. Jensen, S. B. van Berlekom, J. Kajanus, J. Mårtensson and B. Albinsson, *J. Phys. Chem. A*, 1997, **101**, 2218; A. Osuka, N. Tanabe, S. Kawabata, I. Yamazaki and Y. Nishimura, *J. Org. Chem.*, 1995, **60**, 7177; S. Kawabata, I. Yamazaki, Y. Nishimura and A. Osuka, *J. Chem. Soc., Perkin Trans. 2*, 1997, 479.
13 (*a*) P. N. Taylor, A. P. Wylie, J. Huuskonen and H. L. Anderson, *Angew. Chem., Int. Ed. Engl.*, 1998, **37**, 986; (*b*) B. Jiang, S.-W. Yang, D. C. Barbini and W. E. Jones, Jr., *Chem. Commun.*, 1998, 213.
14 D. Lexa, M. Momenteau, J. Mispelter and J.-M. Savèant, *Inorg. Chem.*, 1989, **28**, 30; K. M. Kadish, M. M. Franzen, B. C. Han, C. Araullo-McAdams and D. Sazou, *J. Am. Chem. Soc.*, 1991, **113**, 512; K. M. Kadish, D. Sazou, Y. M. Liu, A. Saoiabi, M. Ferhat and R. Guilard, *Inorg. Chem.*, 1988, **27**, 1198.
15 H. Imahori, H. Higuchi, Y. Matsuda, A. Itagaki, Y. Sakai, J. Ojima and Y. Sakata, *Bull. Chem. Soc. Jpn.*, 1994, **67**, 2500.
16 K. M. Kadish, M. M. Franzen, B. C. Han, C. Araullo-McAdams and D. Sazou, *Inorg. Chem.*, 1991, **31**, 4399.
17 D. P. Arnold, V. V. Borovkov and G. V. Ponomarev, *Chem. Lett.*, 1996, 485.
18 V. V. Borovkov, G. V. Ponomarev, A. Ishida, T. Kaneda and Y. Sakata, *Chem. Lett.*, 1993, 1409; H. Higuchi, K. Shimizu, J. Ojima, K. Sugiura and Y. Sakata, *Tetrahedron Lett.*, 1995, **36**, 5359.
19 M. Chachisvilis, V. S. Chirvony, A. M. Shul'ga, B. Källebring, S. Larsson and V. Sundström, *J. Phys. Chem.*, 1996, **100**, 13857.
20 R. Kitagawa, Y. Kai, G. V. Ponomarev, K. Sugiura, V. V. Borovkov, T. Kaneda and Y. Sakata, *Chem. Lett.*, 1993, 1071.
21 D. P. Arnold, G. A. Heath, G. V. Ponomarev and D. V. Yashunsky, manuscript in preparation.
22 D. Beljonne, G. E. O'Keefe, P. J. Hamer, R. H. Friend, H. L. Anderson and J. L. Brédas, *J. Chem. Phys.*, 1997, **106**, 9439.
23 R. Stranger, J. E. McGrady, D. P. Arnold, I. Lane and G. A. Heath, *Inorg. Chem.*, 1996, **35**, 7791.
24 Z. Wang, P. N. Day and R. Pachter, *J. Chem. Phys.*, 1998, **108**, 2504.
25 S. G. DiMagno, V. S.-Y. Lin and M. J. Therien, *J. Am. Chem. Soc.*, 1993, **115**, 2513.
26 M. Gouterman, in *The Porphyrins*, ed. D. Dolphin, Academic Press, New York, 1978, vol. III, ch. 1; R. A. Binstead, M. J. Crossley and N. S. Hush, *Inorg. Chem.*, 1991, **30**, 1259.
27 See, for example, N. Kobayashi, H. Lam, W. A. Nevin, P. Janda, C. C. Leznoff, T. Koyama, A. Monden and H. Shirai, *J. Am. Chem. Soc.*, 1994, **116**, 879 and references therein.
28 B. D. Yeomans, D. G. Humphrey and G. A. Heath, *J. Chem. Soc., Dalton Trans.*, 1997, 4153; D. C. Ware, M. M. Olmstead, R. Wang and H. Taube, *Inorg. Chem.*, 1996, **35**, 2576.
29 L. Jaquinod, O. Siri, R. G. Khoury and K. M. Smith, *Chem. Commun.*, 1998, 1261; C. K. Johnson and D. Dolphin, *Tetrahedron Lett.*, 1998, **39**, 4753.
30 C. M. Duff and G. A. Heath, *Inorg. Chem.*, 1991, **30**, 2528.

Received in Cambridge, UK, 3rd July 1998;
Paper 8/05087B